ISSN 1063-7729, Astronomy Reports, 2014, Vol. 58, No. 11, pp. 808–824. © Pleiades Publishing, Ltd., 2014.
Original Russian Text © E.I. Staritsin, 2014, published in Astronomicheskii Zhurnal, 2014, Vol. 91, No. 11, pp. 914–932.

# Enhancement of Surface Helium Abundance in Intermediate-Mass Main-Sequence Stars

**E. I. Staritsin***

*K.A. Barchatova Kourovka Astronomical Observatory,*
*B.N. Yeltsin Ural Federal University,*
*Ekaterinburg, Russia*

Received January 22, 2014; in final form, May 21, 2014

**Abstract**—The evolution of rapidly rotating 8, 4, and 2 $M_\odot$ main-sequence stars is considered together with hydrodynamical transfer in their interiors. The conditions under which turbulent erosion, semi-convection, and shear turbulence lead to partial mixing of the matter in the radiative envelope and central regions of the stars are determined. The enhancement of the surface helium abundance with time depends on both the intensity of partial mixing in their interiors and mass loss by the stellar wind. The ratio of the number densities of helium and hydrogen at the surface can rise by the end of main-sequence stage by $\sim$30% for a 8 $M_\odot$ star and $\sim$10–20% for a 4 $M_\odot$ star, depending on the mass-loss rate. Partial mixing of the matter in the radiative envelope and in the central region of the star can provide an explanation for the observed enhancement of the atmospheric helium abundances of early B stars toward the end of their main-sequence evolution. The enhancement of the surface helium abundance in a 2 $M_\odot$ star is so small that it cannot be detected, and is appreciably lower than the enhancement beneath the surface.

**DOI:** 10.1134/S1063772914110055

## 1. INTRODUCTION

The modern theory of stellar structure and evolution provides a fairly deep understanding of a large number of observed features of stars at different stages of their evolution [1–3]. Relatively unstudied questions include the evolutionary significance of hydrodynamical mass transfer in stellar interiors. Various hydrodynamical processes resulting in partial or complete mixing can act in the different layers of a star. The location of the boundaries between the regions where different mixing mechanisms act and the degree of mixing of layers with different chemical compositions are a subject of study. Complete or partial mixing of different layers is reflected in a star's structure, its observed features, and their temporal variations. Cases when the mixing region encompasses layers where nuclear burning is possible are especially interesting. Even incomplete mixing of these and other layers may enable an outflow of nuclear fuel from layers where the physical conditions for nuclear reactions are not satisfied and the inflow of nuclear-burning products into these layers.

The discovery of boron abundances with lower than solar [4] and interstellar [5] values in the atmospheres of main-sequence 8 $M_\odot \leq M \leq 15$ $M_\odot$ B stars provides evidence for partial mixing of the matter in the radiative envelopes of these stars [6–8]. Boron is depleted in nuclear reactions at temperatures $\sim 6 \times 10^6$ K and higher. Such temperatures are reached in relatively shallow layers of such stars. Partial mixing of these and higher-lying layers can already decrease the surface abundance of boron in the early stages of stellar evolution along the main-sequence [9].

The enhanced helium and nitrogen abundances in the atmospheres of main-sequence B stars may provide evidence for mixing with various intensities encompassing the entire star [10–12]. The atmospheric helium abundances of 100 B0–B5 stars were derived in [13]. This sample did not include spectroscopic binaries, pulsating stars, peculiar stars with diminished abundance of He, and Be stars. During main-sequence evolution, the ratio of the number densities of helium and hydrogen atoms $N_{\rm He}/N_{\rm H}$ in the atmospheres of stars with masses 4 $M_\odot \leq M \leq$ 12 $M_\odot$ increases by $26 \pm 10$%, and can reach $\sim$67% for 12 $M_\odot \leq M \leq 19$ $M_\odot$ stars. The atmospheric helium abundances of 326 B stars from 19 young open clusters were determined in [14]; after excluding binaries and chemically peculiar stars, the increases in the helium abundances with time in 88 B0–B2 stars with masses in the range 8 $M_\odot \leq M \leq 16$ $M_\odot$ were found to be $23 \pm 13$% during their main-sequence evolution. Most stars later than B2 had not finished contracting to the zero-age main-sequence [14]. The atmo-

*E-mail: Evgeny.Staritsin@urfu.ru

spheric helium abundances in more massive O stars (masses $M \geq 25\ M_\odot$) can increase by about a factor of two during their main-sequence lifetimes [15–17].

It was suggested [18] that the enhanced atmospheric helium abundances of peculiar B stars may result from the processes in the stellar wind; namely that the stellar wind takes away only some of the helium of the stellar atmospheric material, with the remaining helium falling back onto the star, creating a helium excess in the stellar atmosphere. The stellar winds of hot main-sequence stars form due to the absorption of stellar radiation in lines of heavy ions, with the subsequent transfer of momentum from heavy ions to protons and helium ions via Coulomb interactions [19].

The stellar winds of early B stars have low densities, making a drift of heavy elements relative to the main mass of the hydrogen and helium gas possible, as well as a drift of the protons relative to the helium ions. This drift results in friction between the different elemental components of the wind [20, 21]. In the winds of B stars with effective temperatures exceeding ~15 000 K, helium located close to the star is predominantly singly ionized [18, 22]. If the abundances of heavy elements are solar, the helium is singly ionized, and the friction between the proton and helium components is taken into account, the helium can be accelerated to velocities exceeding the escape velocity [22]. Thus, processes in the stellar wind cannot be the reason for the variation of the relative abundances of hydrogen and helium in the atmospheres of B stars.

One more signature of mixing in stellar interiors is the width of the main sequence and some properties of the locations of open clusters stars in the Hertzsprung–Russell diagram [23–26]. In standard calculations of the evolution of main-sequence B stars, central regions of the star where the local criterion of convective instability is satisfied are taken to be fully mixed [1–3]. All the hydrogen mass in this region is available for nuclear reactions in the very center of the star. Therefore, in such calculations, the mass of helium synthesized during the main-sequence evolution is determined by the size of the region where the local criterion for convective instability is satisfied. However, this mass is not sufficient to explain the width of the main sequences in open clusters.

Thus, the abundances of elements that could be fuel or products of nuclear reactions in stellar interiors in the hydrogen-burning stage that are observed in the stellar atmospheres, and also the observed color–magnitude diagrams of open clusters, serve as indicators of mixing in the interiors of main sequence stars.

In addition to convection, there are other hydrodynamical processes associated with full or partial mixing act in the stellar interiors, such as turbulent entrainment [27], semi-convection [28], meridional circulation [29, 30], and shear turbulence due to the non-rigid rotation of the star [31]. Computations of the evolution of rotating stars taking into account the hydrodynamical processes associated with this rotation provided an explanation for the observed increase in the helium abundances in stars more massive than ~25 $M_\odot$ [32], but such an increase in the helium abundance was not obtained in the computations for lower-mass stars [33, 34].

O stars intensively lose mass via their stellar winds [35]. In the most massive stars, layers with variable chemical composition may already arrive at the stellar surface in the main-sequence stage [36]. Further mass loss uncovers layers with enhanced helium abundances. The mass-loss rates of main-sequence B stars are significantly lower [37, 38], making it impossible for layers of variable chemical composition to appear at the surface due to mass-loss via the stellar wind. The helium abundance at the stellar surface may increase in this case due to partial mixing of the material in the outer layers of the star with layers with variable chemical composition, or with material in the central regions that are fully mixed. In our present study, we investigated the conditions for such mixing in the interiors of 8, 4, and 2 $M_\odot$ stars.

## 2. HYDRODYNAMICAL MODEL FOR MIXING IN THE INTERIOR OF A ROTATING STAR

The hydrodynamical model for mixing in the interior of a rotating star describes the transport of chemical elements and momentum in the vertical direction. The model includes turbulent entrainment, meridional circulation, shear turbulence, and semi-convection. It is assumed that, due to the anisotropy of the turbulence, the star is in a state of shellular rotation [31, 39]. The rotational angular velocity $\Omega(r)$ varies in the vertical direction, depending on mean distance to a surface of constant pressure, and is approximately constant at every such surface.

### *2.1. Turbulent Entrainment*

The central regions of main-sequence stars with $M > 1.5\ M_\odot$ are convective. In standard calculations, the radius of the convective region is determined using the local criterion for convective instability [1–3]. According to this criterion, this region is surrounded by layers that are stable against convection. The motion of matter in the zone of convective instability is turbulent. The matter of the rising turbulent flow spreads in a horizontal plane in the vicinity of the boundary of the turbulent region and

then descends, flowing around the upward-flowing stream. In the region of horizontal flow, the velocities of different layers located one above the other vary in the vertical direction. This shear flow involves higher-lying layers that are stable to convection in this motion, bringing their matter inside the turbulent region. The interface between the convectively turbulent region and stable layers moves along the stable layers due to the continuous involvement of new layers in the turbulent motion. The velocity of the interface moving along the matter of the stable layers $V_e$ is determined by the law of turbulent entrainment

$$V_e/V_t = A\mathrm{Ri_B}^{-n}, \quad (1)$$

where $V_t$ is the typical velocity of the turbulent pulsations near the interface, $n$ and $A$ are parameters of the turbulent entrainment law,

$$\mathrm{Ri_B} = \frac{\triangle b\ell}{V_t^2}$$

is the bulk Richardson number, $\ell$ is the largest size of the turbulent eddies,

$$\triangle b = \int_h N^2 dr$$

is the buoyancy jump across the interface, $N$ is the local frequency of the buoyancy, $h \sim V_c/N$, and $V_c$ is the convective velocity.

In the case of turbulent entrainment, the value of $n$ at the boundaries of the convective cores of main-sequence stars has been found via 3D numerical modeling of convective turbulence in the stellar interiors: $n = 1.05 \pm 0.21$ [27]. The typical turbulent-pulsation velocity $V_t$ is related to the rate of dissipation of the kinetic energy of the turbulent motion in the stellar interiors $\epsilon_k$ via the well known Kolmogorov relation [40, 41]. A model for determining $\epsilon_k$ using the results of 1D computations was suggested in [42]. This model can be used to successively determine $\epsilon_k$, $V_t$, $V_e$, and the distance $d$ from the boundary of the zone where the local condition for convective instability is satisfied to the boundary of the zone of convective turbulence [43]:

$$d = V_e \triangle t, \quad (2)$$

where $\triangle t$ is the time step in the numerical computations for the stellar evolution. Convective turbulence promotes a uniform chemical composition in the central regions of the star [27]. The distance $d$ is usually measured in terms of the pressure scale height $H_P$ at the boundary of the region where the local condition for convective instability is satisfied; $\alpha = d/H_P$ [24]. We assumed that the region of convective turbulence rotates rigidly.

### 2.2. Meridional Circulation and Shear Turbulence

The vertical transport of momentum in the outer layers of the star located above the region of convective turbulence due to meridional circulation and shear turbulence is determined by momentum conservation [44]:

$$\frac{\partial(\rho\varpi^2\Omega)}{\partial t} + \mathrm{div}(\rho\varpi^2\Omega\mathbf{u}) = \mathrm{div}(\rho\nu_\mathrm{v}\varpi^2\mathrm{grad}\Omega), \quad (3)$$

where $\rho$ is density, $\varpi$ the distance to the rotation axis, $t$ time, $\mathbf{u}$ the velocity of the meridional circulation, and $\nu_\mathrm{v}$ the turbulent viscosity in the vertical direction. The solution of (3) enables the determination of the distribution of the rotational angular velocity.

In the case of shellular rotation, the vertical component of the meridional circulation can be written [31]

$$U_r(r,\theta) = U(r)P_2(\theta),$$

where $U(r)$ is the amplitude of the vertical component of the meridional-circulation velocity and $P_2(\theta)$ the second order Legendre polynomial. The amplitude $U(r)$ can be found from the condition for energy conservation in the stationary case [31, 45]:

$$\rho T\mathbf{u}\mathrm{grad}s = \rho\varepsilon_n + \mathrm{div}(\chi\mathrm{grad}T) - \mathrm{div}\mathbf{F}_h, \quad (4)$$

where $T$ is the temperature, $s$ the specific entropy, $\varepsilon_n$ the rate of nuclear energy release, $\chi$ the thermal conductivity, $\mathbf{F}_h = -\nu_h\rho T\partial s/\partial\mathbf{i}_\theta$ the turbulent enthalpy flux in the horizontal direction, and $\nu_h$ the turbulent viscosity in the horizontal direction, i.e., along a surface of constant pressure.

### 2.3. Semi-convection

A linear analysis of the stability of a gaseous medium with radiation shows that the medium is unstable if [46]

$$\nabla_a \le \nabla \le \nabla_a + \frac{\beta}{4-3\beta}\nabla_\mu,$$

where $\nabla$ is the temperature gradient, $\nabla_a$ the adiabatic temperature gradient, $\nabla_\mu$ the mean molar-mass gradient, and $\beta$ the ratio of the gas to the total pressure.

In models of non-rotating main-sequence stars, such instability arises in the layer with variable chemical composition that forms during the evolution of a massive star ($M > 10\ M_\odot$), due to the decrease of the mass of the convective core. This instability leads to partial mixing in the layer with variable chemical composition. Unlike models for turbulent entrainment, detailed models of this mixing have not yet been developed. As a result of partial mixing, semi-convection, a neutral state relative to the instability can arise in the layer of variable chemical

composition. Two criteria for neutrality in the semi-convective zone have been put forward. One is the S criterion [28]:

$$\nabla = \nabla_a \tag{5}$$

and the other, proposed [47], is the L criterion [48]:

$$\nabla = \nabla_a + \frac{\beta}{4-3\beta}\nabla_\mu.$$

Semi-convection mixes the matter in the layer with variable chemical composition, but does not transport momentum as efficiently as meridional circulation [49]. The mixing is strongest if the S criterion is chosen.

### 2.4. Transport of Chemical Elements

The transport of hydrogen mass is described by the diffusion equation [50]

$$\frac{\partial(\rho X)}{\partial t} = \mathrm{div}(\rho D \mathrm{grad} X). \tag{6}$$

Here, $X$ is the mass abundance of hydrogen, and the diffusion coefficient $D$ is defined as the sum $D = D_\mathrm{v} + D_{sc}$, where $D_\mathrm{v}$ is the vertical turbulent-diffusion coefficient and $D_{sc}$ is the diffusion coefficient associated with semi-convection.

The turbulent viscosity $\nu_t$ and diffusion $D_t$ coefficients are different in different flows, and can vary by several orders of magnitude within a flow, but their ratio, the turbulent Schmidt number

$$\mathrm{Sc}_t = \nu_t/D_t \tag{7}$$

varies only weakly within a specific flow and from flow to flow [51, 52]. Meridional circulation transports elements in the vertical direction inefficiently compared to shear turbulence [49].

### 2.5. Turbulent Viscosity Coefficients

The vertical turbulent-viscosity coefficient is defined by the condition that the work done by gravity during the interchange of two arbitrary fluid parcels and the excess kinetic energy in the stream be equal, taking into account the destabilizing roles of the energy exchange between the parcel and the surrounding matter due to re-radiation of photons and the transfer of chemical elements in the horizontal direction due to the anisotropy of the turbulence. The vertical turbulent-viscosity coefficient is [53]:

$$\nu_\mathrm{v} = \frac{2\mathrm{Ri}_c}{N_T^2/(K+D_h) + N_\mu^2/D_h}\left(\frac{d(\varpi\Omega)}{dr}\right)^2, \tag{8}$$

where $K = 4acT^3/3c_P\rho^2\kappa$, $N_T^2 = (g\delta/H_p)(\nabla_a - \nabla)$, $N_\mu^2 = (g/H_p)\nabla_\mu$, $N^2 = N_T^2 + N_\mu^2$, $\mathrm{Ri}_c$ is the critical value of the local Richardson number, $D_h$ the horizontal turbulent-diffusion coefficient, $a$ Stefan's constant, $c$ the speed of light, $c_P$ the specific heat capacity at constant pressure, $\kappa$ the opacity, $g$ the average gravitational acceleration on a constant-pressure surface, and $\delta = (4-3\beta)/\beta$.

The horizontal turbulent-viscosity coefficient is derived from the condition that the transport of momentum through a constant-pressure surface by meridional circulation be equal to the shear turbulence along the same surface [31]:

$$\nu_h \sim C_z r\,|U(r)|\,. \tag{9}$$

The parameter $C_z$ incorporates the ratio of the amplitude of the variation of the angular velocity at the constant-pressure surface and the average angular velocity at the same surface, assumed to be $\sim$1. However, the turbulence-anisotropy condition is not satisfied when $C_z \sim 1$ [54]. Two other expressions for the horizontal turbulent-viscosity coefficient can be derived by considering the rate of dissipation of the excess kinetic energy in the turbulent flow [55], or based on measurements of the torque in classical Couette–Taylor experiments [56]. In both cases, the results exceed the coefficient derived using Eq. (9) with $C_z \sim 1$ by two orders of magnitude. However, in each case, the expression for the coefficient contains a free parameter. Therefore, we used Eq. (9) to determine the horizontal turbulent-viscosity coefficient. The value of $C_z$ was chosen so that the condition for validity of (9) is satisfied [31]:

$$\nu_\mathrm{v} \ll \nu_\mathrm{h} \ll K.$$

### 2.6. Parameters of the Hydrodynamical Model for Mixing in Stellar Interiors

Our modern model for mixing in stellar interiors contains the free parameters $C_z$ in the expression for the horizontal turbulent-viscosity coefficient, the turbulent Schmidt number $\mathrm{Sc}_t$ relating the turbulent-viscosity and diffusion coefficients, $A$ in the turbulent-entrainment law, and the extent of mixing in the semi-convective zone. The parameters $\mathrm{Sc}_t$ and $A$ are usually derived using experimental data [51, 52, 57]. These parameters should also be constrained by observations in studies of stellar evolution. The pattern of mixing in the semi-convective zone must be determined using 3D hydrodynamical calculations. The analysis of such computations may enable the construction of a model for mixing in the semi-convective zone, as was done for turbulent entrainment [42]. Additional studies are probably necessary to determine the horizontal turbulent-viscosity coefficient [56].

Thus, this modern model for mixing in stellar interiors can be used for studies of the evolution of rotating stars, but must be constrained by observations and itself requires additional studies.

Stellar masses, parameters of the mixing model, and some characteristics of the structure and evolution of main-sequence stars

| $M$, $M_\odot$ | $\mathrm{Sc}_t$ | Criterion | $\alpha_0$ | $(\Omega_c/\Omega_s)_0$ | $X_c^{\mathrm{beg}}$ | $X_c^{\mathrm{cont}}$ | $\Delta M_{\mathrm{He}}$, $M_\odot$ | $t_{MS}$, $10^6$ yr | $\Delta M_{\mathrm{lost}}$, $M_\odot$ |
|---|---|---|---|---|---|---|---|---|---|
| 8 | 0.1 | S | 0.05 | 1.23 | 0.59 | 0.56 | 2.23 | 36.8 | 0.0103 |
| 8 | 0.3 | S | 0.05 | 1.23 | 0.47 | 0.20 | 1.26 | 29.1 | 0.0026 |
| 8 | 1.0 | S | 0.05 | 1.23 | – | – | 1.21 | 28.3 | 0.0024 |
| 8 | 0.1 | – | 0.05 | 1.23 | – | – | 1.21 | 28.3 | 0.0024 |
| 8 | 0.1 | S | 0.15 | 1.21 | 0.40 | 0.36 | 1.91 | 35.3 | 0.0066 |
| 8 | 0.1 | S | 0.25 | 1.19 | 0.22 | 0.15 | 1.67 | 32.9 | 0.0048 |
| 4 | 0.1 | S | 0.05 | 1.38 | 0.56 | 0.50 | 0.57 | 147.7 | (?) |
| 2 | 0.1 | S | 0.05 | 1.48 | 0.27 | 0.17 | 0.19 | 877.8 | 0.0 |

## 3. STELLAR-WIND MASS LOSS

We determined the mass-loss rates in the evolutionary computations for a 8 $M_\odot$ star applying the interpolation formula from [58], which is based on observational data. Theoretical mass-loss rates by main-sequence B stars were computed in [38]. A system of statistical-equilibrium equations was solved in [38] to determine the ionization and excitation states of different atoms. Computed mass-loss rate of a solar-composition 7.84 $M_\odot$ star is consistent with the estimate based on the formula of [58]. With decrease in the stellar mass, the density of the stellar wind decreases, making the interaction of heavy ions with protons and helium ions become less efficient. If the mass of a star is below $\sim$4 $M_\odot$, these interactions become so weak that the ejection of hydrogen and helium becomes impossible. Thus, 4 $M_\odot$ represents a lower limit for the mass of hot stars possessing stellar winds. We computed the evolution of a 4 $M_\odot$ star assuming the minimum mass-loss rate provided by the computations [38].

## 4. PARTIAL MIXING IN THE STELLAR INTERIORS

Partial mixing in the interior of a rotating star is due to the simultaneous action of several mixing processes in different regions of the star. Turbulent entrainment acts at the boundary of the region of convective turbulence, and turbulent diffusion in non-convective regions of the star. Semi-convection may act in the layer with variable chemical composition that forms above the region of convective turbulence in the course of the star's evolution. Partial mixing in stellar interiors depends on the intensity of each of these processes and the mass of the star. The intensity of mixing by turbulent diffusion is specified by the turbulent Schmidt number $\mathrm{Sc}_t$. The intensity of mixing in the semi-convective zone is specified by our selection of the neutrality criterion relative to to semi-convection. The location of the region of convective turbulence depends on $A$, which may be replaced by the initial value of $\alpha$.

We studied the evolution of 8, 4, and 2 $M_\odot$ stars in the core-hydrogen-burning stage for various sets of these parameters (see the table). Equations (1)–(9) were solved together with the stellar-structure equations. We used the mass of matter below a constant-pressure surface as an independent variable. The code of Paczyński [59] was used for our computations, modified to take into account the influence of rotation on the stellar structure [60] and to include various hydrodynamical transport processes [43, 49, 61, 62]. We specified the initial chemical compositions of the stars to be close to solar: $(X, Z) = (0.70, 0.02)$, where $X$ and $Z$ are the mass abundances of hydrogen and heavy elements. We used the opacity tables of [63] for the high-temperature region ($\log T \geq 4.0$) and those of [64] for the low-temperature region ($\log T < 4.0$). The parameter $C_z$ was set to $10^2$, for which the horizontal turbulent-viscosity coefficient $\nu_h$ is about two orders of magnitude higher than the vertical turbulent-viscosity coefficient, and the maximum value of $\nu_h$ is about half an order of magnitude lower than $K$. The critical value of the local Richardson number $\mathrm{Ri}_c$ was set to 1/4.

The difference of the angular velocities at the boundary of the region of convective turbulence and the stellar surface in the initial model of the evolutionary sequence $(\Omega_c/\Omega_s)_0$ was selected so that the time scale for angular-momentum transport by meridional circulation was equal to the nuclear time scale of the star [61, 62]. In all cases, the equatorial angular velocity was set to 250 km/s. The angular momentum was then equal to $6.94 \times 10^{51}$,

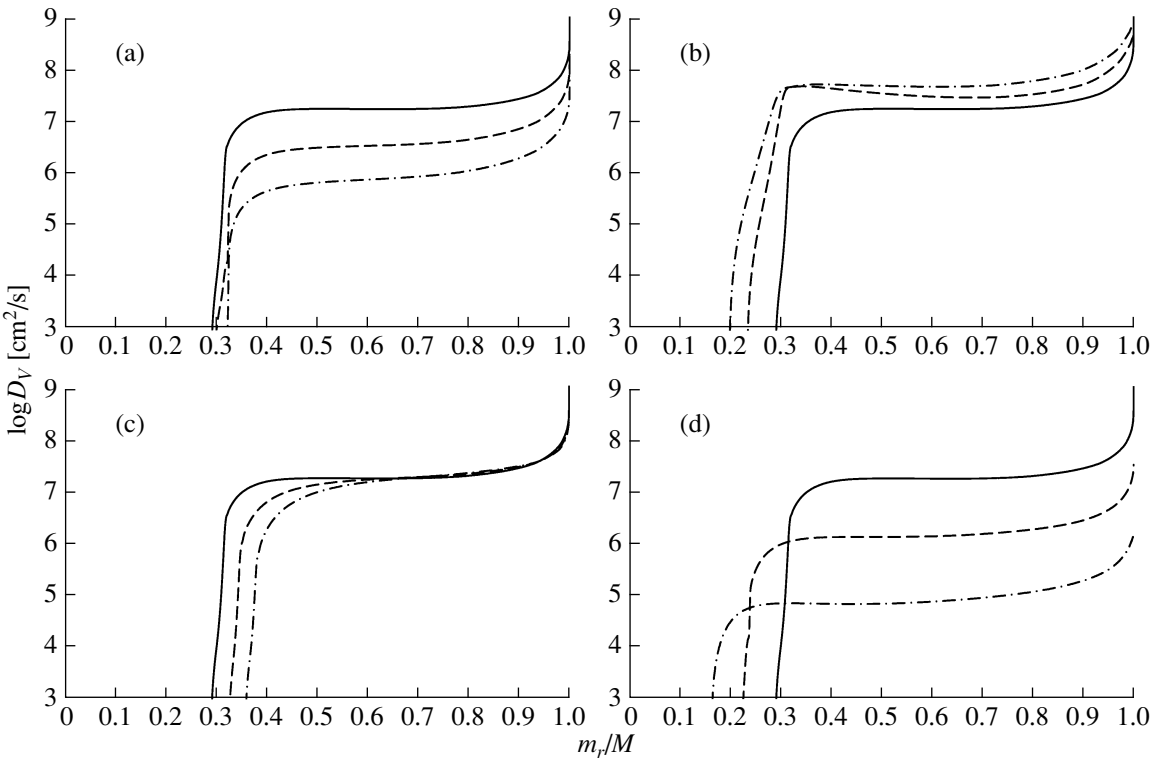


**Fig. 1.** Dependence of the diffusion coefficient associated with shear turbulence $D_V$ on the Lagrangian coordinate $m_r/M$: (a) in the interior of an 8 $M_\odot$ star evolving with $\mathrm{Sc}_t = 0.1$ (solid), $\mathrm{Sc}_t = 0.3$ (dashed), $\mathrm{Sc}_t = 1.0$ (dot–dashed), satisfying the S-criterion for semi-convection, and with $\alpha_0 = 0.05$ when the hydrogen abundance in the region of convective turbulence is $X_c \sim 0.6$; (b) in the interior of an 8 $M_\odot$ star evolving with $\mathrm{Sc}_t = 0.1$, satisfying the S-criterion for semi-convection, and with $\alpha_0 = 0.05$ when the hydrogen abundance in the region of convective turbulence is $X_c \sim 0.6$ (solid), $X_c \sim 0.4$ (dashed), and $X_c \sim 0.2$ (dot–dashed); (c) in the interior of an 8 $M_\odot$ star with $\mathrm{Sc}_t = 0.1$, satisfying the S-criterion for semi-convection, and with $\alpha_0 = 0.05$ (solid), $\alpha_0 = 0.15$ (dashed), and $\alpha_0 = 0.25$ (dot–dashed) when the hydrogen abundance in the region of convective turbulence is $X_c \sim 0.6$; (d) in the interiors of 8 $M_\odot$ (solid), 4 $M_\odot$ (dashed), and 2 $M_\odot$ (dot–dashed) stars evolving with $\mathrm{Sc}_t = 0.1$, satisfying the S-criterion for semi-convection, and with $\alpha_0 = 0.05$ when the hydrogen abundance in the region of convective turbulence is $X_c \sim 0.6$. The behavior of the turbulent-diffusion coefficient in a sub-surface layer with mass $\sim 6 \times 10^{-4}$ $M_\odot$ is not shown.

$2.02 \times 10^{51}$, and $0.55 \times 10^{51}$ erg s for the 8, 4, and 2 $M_\odot$ stars, respectively.

### *4.1. Role of Shear Turbulence*

In gas streams that are in a state of free turbulent flow, the efficiency of the turbulent transport of elements is higher than the efficiency of the turbulent transport of angular momentum. Therefore, the turbulent Schmidt number in such streams is lower than unity [51, 52]. Numerous experimental and theoretical estimates of the turbulent Schmidt number have shown that it is approximately constant in regions of developed turbulence with shear, but can vary within 0.1 to 1.0 from flow to flow, depending on the presence of external force fields, temperature gradients, and the total amount of admixture in the stream [65].

In the 8 $M_\odot$ stars, the vertical turbulent-diffusion coefficient $D_V$ is approximately constant in the bulk of the region involved in the shear turbulence. The value of this coefficient depends on the turbulent Schmidt number (Fig. 1a) and the time (Fig. 1b). The coefficient decreases sharply in the layer of variable chemical composition due to the decrease of the typical size of the turbulent eddies [53, 66]. The behavior of the coefficient in the sub-surface layer is described in detail in Section 4.3.

The time scale for mixing in the layer between the constant-pressure surface located an average distance $r$ from the stellar center and the stellar surface, located at the distance $R$, $t_{\mathrm{mix}}$, can be estimated using formula [67]:

$$t_{\mathrm{mix}} \sim \frac{(R-r)^2}{6D_V(r)}.$$

The ratio of the mixing time scale $t_{\mathrm{mix}}$ and the remaining main-sequence evolution time $t_{MS} - t$ for an 8 $M_\odot$ star is shown in Fig. 2 for various Schmidt numbers.

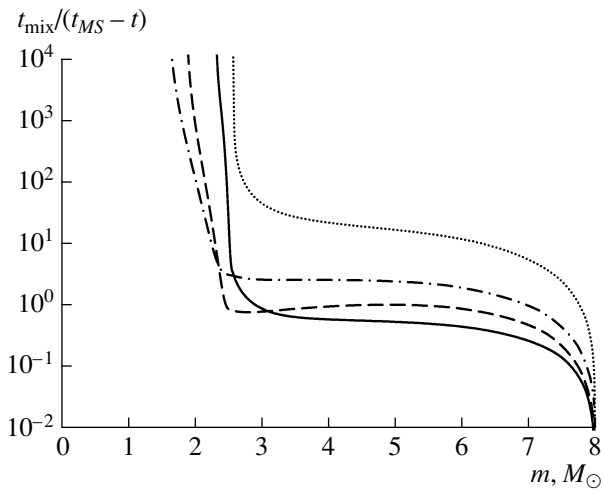


**Fig. 2.** Ratio of the time scale for mixing by turbulent diffusion $t_{\rm mix}$ and the remaining evolution time on the main sequence $t_{MS} - t$ in the interior of an 8 $M_\odot$ star with $\mathrm{Sc}_t = 0.1$ at times $t$ when the hydrogen abundance in the region of convective turbulence is $X_c \sim 0.6$ (solid), $X_c \sim 0.4$ (dashed), and $X_c \sim 0.2$ (dot–dashed) and with $\mathrm{Sc}_t = 1.0$ at the time when $X_c \sim 0.6$ (dotted). The S-criterion for neutrality was applied in the semi-convective zone; $\alpha_0 = 0.05$.

With $\mathrm{Sc}_t = 0.1$, the mixing time scale in the stellar envelope is comparable to order of magnitude with the remaining evolutionary time over the total main-sequence lifetime of the star. As the star evolves, the mixing time scale increases slightly relative to the remaining evolution time, despite the increase in the diffusion coefficient (Fig. 1b). This is due both to the reduction of the remaining evolutionary time and the increase in the size of the stellar envelope due to its expansion. The mixing time scale in the layer of variable chemical composition is significantly longer than the main-sequence lifetime of the star. Shear turbulence transports hydrogen from the initially chemically homogeneous envelope to the upper part of the layer with variable chemical composition. Accordingly, helium is transported in the opposite direction. The turbulent flux of hydrogen is strongly reduced in the layer of variable chemical composition (Fig. 3a).

### *4.2. Role of Semi-Convection*

Due to the increase in the hydrogen abundance in the upper part of the layer with variable chemical composition, the conditions for semi-convection may arise there. The lower boundary of the semi-convective zone descends into the stellar interior, and may reach the region of convective turbulence. The appearance of semi-convection and the possibility of contact between the semi-convective zone and the region of convective turbulence are determined by the mass of hydrogen that is transported into the layer of variable chemical composition from higher-lying layers.

In the 8 $M_\odot$ stars, the flux of hydrogen in the region of shear turbulence is higher for $\mathrm{Sc}_t = 0.1$ than for $\mathrm{Sc}_t = 0.3$. Therefore, the conditions for semi-convection arise earlier with $\mathrm{Sc}_t = 0.1$, when the hydrogen abundance in the region of convective turbulence $X_c^{\rm beg}$ is higher, and the lower boundary of the semi-convective zone descends inside the star to the region of convective turbulence earlier when the hydrogen abundance in the region of convective turbulence $X_c^{\rm cont}$ is higher (see the table). After establishing the contact between the semi-convective zone and the region of convective turbulence, the hydrogen from the semi-convective zone is transported into the region of convective turbulence, while helium is transported in the opposite direction. Thus, if $\mathrm{Sc}_t = \{0.1, 0.3\}$ and semi-convection is included, partial mixing of the matter in the initially chemically homogeneous radiative envelope and the mater in the region of convective turbulence becomes possible (Fig. 3b).

The mixing time scale is significantly longer than the evolutionary lifetime when $\mathrm{Sc}_t = 1.0$ (Fig. 2). The hydrogen flux in the zone of shear turbulence is not high (Fig. 3b). The upper part of the layer of variable chemical composition and the lower part of the chemically homogeneous envelope mix only slightly (Fig. 4a). The conditions for semi-convection in the layer of variable chemical composition do not arise in this case.

When $\mathrm{Sc}_t = 0.1$, the hydrogen abundance in the radiative envelope of an 8 $M_\odot$ star decreases significantly with time, while the helium abundance increases, due to partial mixing of the radiative envelope and the region of convective turbulence (Fig. 4b). Since the hydrogen transported into the region of convective turbulence from the radiative envelope is processed into helium, the total mass of helium in the radiative envelope becomes higher than it would be in the absence of partial mixing. The increase in the helium mass in the radiative envelope leads to an increase in the opacity of the stellar matter in the envelope and, hence, to an increase in the stellar luminosity. Accordingly, the central region of the star where the local criterion for convective instability is satisfied engulfs a larger mass of the star [66]. The mass of the region of convective instability becomes higher than when partial mixing of this region and the radiative envelope is not taken into account, and the difference of the masses of the regions of convective instability in two cases of the evolution increases as the star evolves.

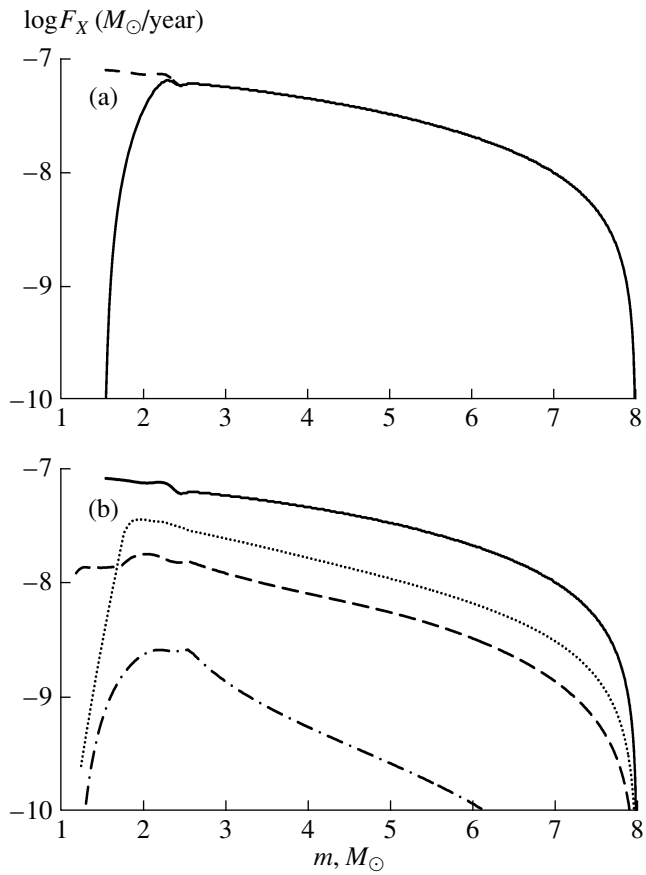


**Fig. 3.** Flux of hydrogen $F_X$ in the interior of an 8 $M_\odot$ star at the time when the hydrogen abundance in the region of convective turbulence $X_c \sim 0.1$. (a) Flux due to shear turbulence (solid) and the total mass flux in the semi-convective zone due to shear turbulence and semi-convection (dashed) with $\mathrm{Sc}_t = 0.1$ and the S-criterion for neutrality for the semi-convective zone. (b) Total flux with $\mathrm{Sc}_t = 0.1$ (solid), $\mathrm{Sc}_t = 0.3$ (dashed) and the S-criterion for neutrality, and the flux due to shear turbulence with $\mathrm{Sc}_t = 1.0$ (dot–dashed) and $\mathrm{Sc}_t = 0.1$ (dotted), without including mixing in the semi-convective zone. In all cases, $\alpha_0 = 0.05$.

The increase in the mass of the region of convective turbulence and the transport of hydrogen into this zone from the radiative envelope increase the mass of synthesized helium and the main-sequence lifetime of the star. When $\mathrm{Sc}_t = 0.1$ and for an 8 $M_\odot$ star, the base of the semi-convective zone contacts the boundary of the region of convective turbulence appreciably earlier than when $\mathrm{Sc}_t = 0.3$, making the mass of synthesized helium $\Delta M_{\mathrm{He}}$ and the main-sequence lifetime $t_{MS}$ considerably larger for $\mathrm{Sc}_t = 0.1$ (see the table).

One case of the evolution of an 8 $M_\odot$ star was computed for $\mathrm{Sc}_t = 0.1$ without mixing in the semi-convective zone. Since the flux of hydrogen in the region of shear turbulence is considerably for this Schmidt number (Fig. 3b), the matter of the radiative envelope mixes with the matter of the upper part of the layer of variable chemical composition (Fig. 4c). In this case, hydrogen from the radiative envelope does not enter the region of convective turbulence, and the amount of nuclear fuel available for helium synthesis does not increase. The helium in the outer layers of the star, located above the region of convective turbulence, is redistributed, but the total mass of the helium in these layers is the same as in the absence of partial mixing. The mass of the matter in the region where the local criterion for convective instability is satisfied varies with time in the same way as when mixing occurs in the region of convective turbulence only. Therefore, the mass of synthesized helium and main-sequence lifetime in this case and in the case of evolution with $\mathrm{Sc}_t = 1.0$ are similar (see the table). However, the distributions of hydrogen and helium in the radiative envelopes of the stars are different in these two cases (Figs. 4a and 4c).

As a result of the action of shear turbulence in the outer layers of the star, helium is transported to the stellar surface. When $\mathrm{Sc}_t = 0.1$, the diffusion wave reaches the surface approximately at the middle of the main-sequence evolution (Fig. 5). If mixing of matter

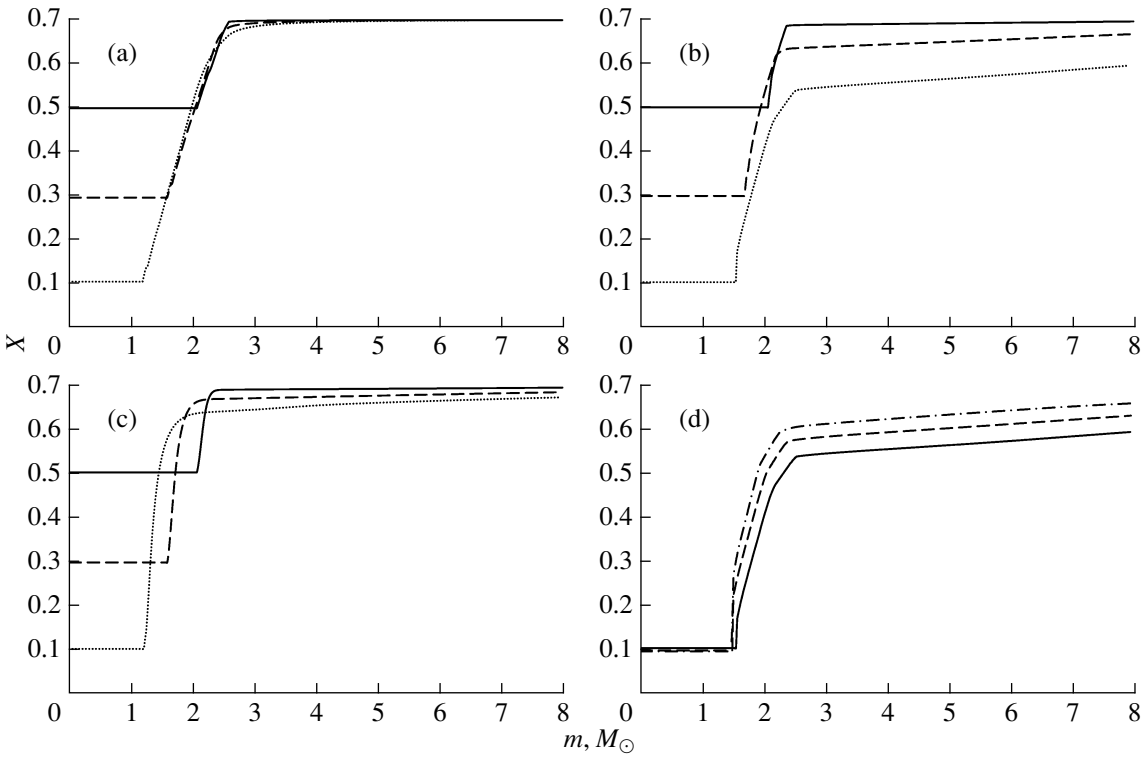


**Fig. 4.** (a, b, c) Distribution of the hydrogen abundance in an 8 $M_\odot$ star at times when hydrogen abundance in the region of convective turbulence $X_c \sim 0.5$ (solid), $\sim 0.3$ (dashed), and $\sim 0.1$ (dotted). Plot (a) is for the case of $\mathrm{Sc}_t = 1.0$ and $\alpha_0 = 0.05$, plot (b) for $\mathrm{Sc}_t = 0.1$ with the S-criterion for neutrality in the semi-convective zone and $\alpha_0 = 0.05$, and plot (c) for $\mathrm{Sc}_t = 0.1$ without mixing in the semi-convective zone and $\alpha_0 = 0.05$. (d) Distribution of hydrogen in an 8 $M_\odot$ star when $X_c \sim 0.1$ for $\mathrm{Sc}_t = 0.1$, the S-criterion for neutrality in the semi-convective zone, and $\alpha_0 = 0.05$ (solid), $\alpha_0 = 0.15$ (dashed), and $\alpha_0 = 0.25$ (dash-dotted).

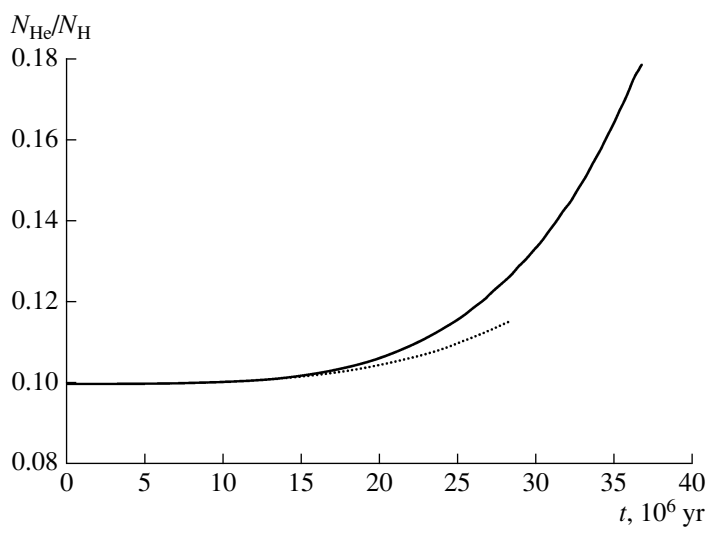


**Fig. 5.** Variation of the ratio of the number densities of helium and hydrogen at the surface of an 8 $M_\odot$ star during its main-sequence evolution when the S-criterion for neutrality is adapted in the semi-convective zone (solid) and when mixing in the semi-convective zone is not taken into account (dotted). In both cases, $\mathrm{Sc}_t = 0.1$ and $\alpha_0 = 0.05$.

in the semi-convective zone is not taken into account, the ratio of the number densities of helium and hydrogen at the stellar surface of an 8 $M_\odot$ star $N_{\rm He}/N_{\rm H}$ increases by the end of the main-sequence lifetime by ~15%. This ratio increases by ~26% during the same time when mixing in the semi-convective zone is included. The structure of the star at the time considered is different in these two cases. When semi-convection is not taken into account, the central region of the star contains the recently formed helium core. When semi-convection is included, the star still burns hydrogen, and the hydrogen abundance in the region of convective turbulence is ~0.24. Since the partial mixing of the matter of the radiative envelope and the region of convective turbulence increases the main-sequence lifetime of the star, $N_{\rm He}/N_{\rm H}$ continues to increase, reaching ~80% at the end of the main-sequence evolution (Fig. 5).

### *4.3. Effect of Mass-Loss*

The behavior of the angular velocity in the sub-surface layer of a star depends on its angular momentum. If the angular momentum of a star is relatively low, the angular velocity monotonically decreases from the boundary of the region of convective turbulence to the stellar surface. If the angular momentum is relatively high, the angular velocity has a minimum beneath the stellar surface and increases slightly toward the surface in the sub-surface layer [54, 62]. For intermediate values of the angular momentum, the minimum of the angular velocity is at the surface at the beginning of the main-sequence evolution, but recedes below the surface with time.

In the case considered of an 8 $M_\odot$ star with an equatorial rotational velocity at the beginning of its evolution of 250 km/s, the angular momentum is in the intermediate range. When the stellar model was evolved with $\mathrm{Sc}_t = 0.1$, mixing in the semi-convective zone was taken into account, and $\alpha_0 = 0.05$, the angular-velocity minimum moves below the surface at an age of ~19 Myr (the hydrogen abundance in the zone of convective turbulence is $X_c \sim 0.43$). By this time, $N_{\rm He}/N_{\rm H}$ has increased by ~1.5%. The angular-velocity minimum continues to move slightly inward in the star during its subsequent evolution. The coefficient of turbulent diffusion vanishes at the constant-pressure surface that rotates with the minimum angular velocity (Fig. 6). Mixing occurs in inner layers of the star, right up to this surface. The mass of the sub-surface layer where the angular velocity increases outward, $\Delta M_{\rm up}$, increases with time, increasing to $\sim 5.0 \times 10^{-4}\ M_\odot$ by the end of the main-sequence evolution. As a result of the shift of the angular-velocity minimum inward in the star, the mixed layers move into the sub-surface layer. Since the coefficient of turbulent diffusion in the sub-surface layer is fairly high (Fig. 6b), the chemical composition

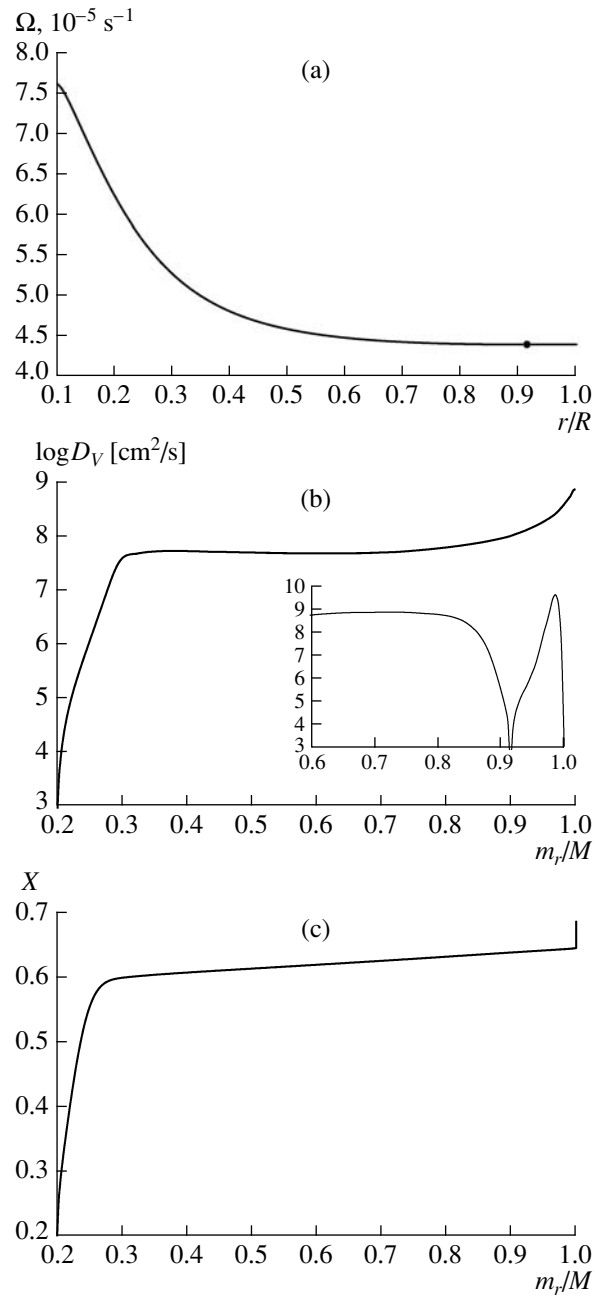


**Fig. 6.** Distributions of various physical parameters in layers of an 8 $M_\odot$ star located outside the region of convective turbulence when the hydrogen abundance in the region of convective turbulence is $X_c \sim 0.2$: (a) angular velocity (the minimum is marked by a circle), (b) vertical coefficient of turbulent diffusion (the behavior of the coefficient in the sub-surface layer with mass ~0.06 $M_\odot$ as a function of relative distance to the center of the star $r/R$ is shown in more detail in the insert; the values $D_V < 10^3$ are not shown), (c) mass abundance of hydrogen. The computations were made for $\mathrm{Sc}_t = 0.1$, applying the S-criterion for semi-convection, and $\alpha_0 = 0.05$. The stellar-wind mass loss was not taken into account.

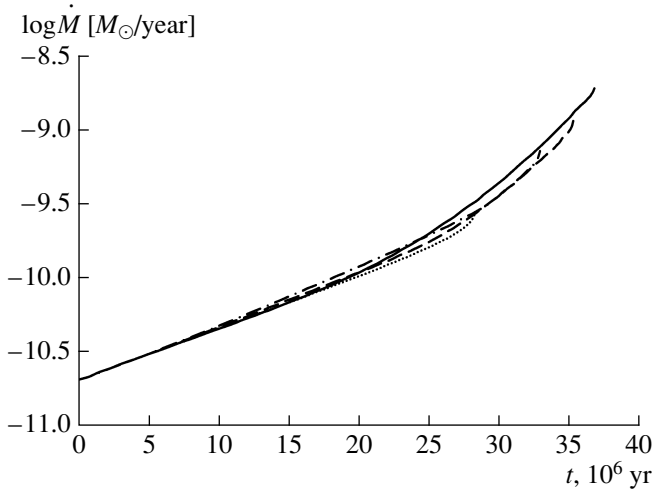


**Fig. 7.** Stellar-wind mass-loss rate from an 8 $M_\odot$ main-sequence star for values of $\mathrm{Sc}_t$ and $\alpha_0$ equal to (0.1, 0.05) (solid), (0.1, 0.15) (dashed), (0.1, 0.25) (dot–dashed), and (1.0, 0.05) (dotted). The S-criterion for semi-convection was applied in all cases.

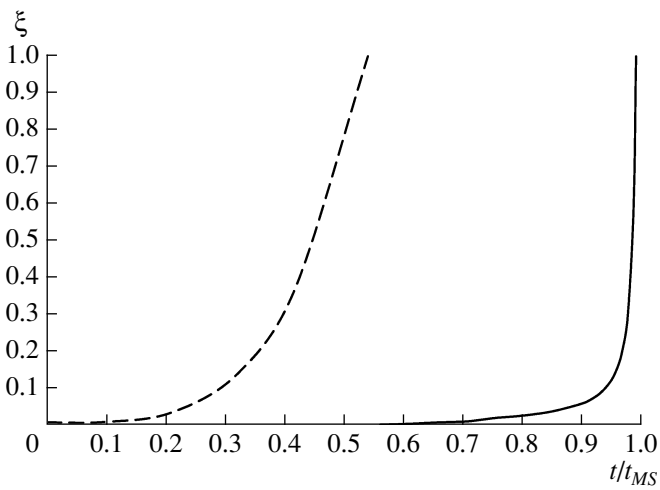


**Fig. 8.** Ratio of the time required to lose the outer layer of a star with mass $\Delta M_{\mathrm{up}}$, in which the angular velocity increases outward, to the remaining main-sequence lifetime, $\xi = (\Delta M_{\mathrm{up}}/\dot{M})/(t_{MS} - t)$, as a function of the relative main-sequence evolution time $t/t_{MS}$ for 8 $M_\odot$ (solid) and 4 $M_\odot$ (dashed) stars with $\mathrm{Sc}_t = 0.1$, the S-criterion for semi-convection, and $\alpha_0 = 0.05$.

of this layer becomes almost homogeneous. If the rate of mass-loss by the star is low, a discontinuity in the chemical composition of the matter below and above the constant-pressure surface that rotates with the minimum angular velocity may arise (Fig. 6c). The sub-surface layers will be mixed to a lesser extent then the matter below them. In the case considered, if mass-loss is not taken into account, $N_{\mathrm{He}}/N_{\mathrm{H}}$ increases by ∼23% at the surface of an 8 $M_\odot$ star by the end of its main-sequence evolution.

If mass-loss is taken into account according to [58], the mass-loss rate for an 8 $M_\odot$ star increases from $2.1 \times 10^{-11}$ $M_\odot$/yr at the beginning of the main-sequence evolution to $2.7 \times 10^{-10}$–$1.9 \times 10^{-9}$ $M_\odot$/yr at the end of this evolution, depending on the scenario for the evolution (Fig. 7). The total mass lost by the star during its main-sequence evolution $\Delta M_{\mathrm{lost}}$ does not exceed 0.15% of the total stellar mass. The time $\Delta M_{\mathrm{up}}/\dot{M}$ required for the loss of a sub-surface layer with mass $\Delta M_{\mathrm{up}}$ increases starting from the time when the angular-velocity minimum moves beneath the stellar surface, and approaches $26 \times 10^4$ yr by the end of the main-sequence evolution. This time is substantially lower than the remaining main-sequence lifetime through the entire lifetime of the star on the main-sequence

(Fig. 8). Therefore, no discontinuity in the chemical composition of the matter in the sub-surface and lower layers forms in an 8 $M_\odot$ star (Fig. 4).

### *4.4. Effect of Turbulent Entrainment*

The law of turbulent entrainment can be used to trace the relative evolution of the thickness of the layer located between the boundaries of the regions of local convective instability and of convective turbulence (Fig. 9). During the star's evolution, the thickness of the layer $d$ decreases with time, since the discontinuity in the buoyancy at the boundary of the region of convective turbulence increases considerably more rapidly than the typical turbulent velocity rates [43]. The thickness of this layer decreases more rapidly than the pressure scale height $H_P$ at the boundary of the region of local convective instability. Therefore, $\alpha = d/H_P$ decreases with time (Fig. 9).

The parameter $A$ in the turbulent-entrainment law can have different values, depending on the conditions for the turbulent flow [57]. $\alpha$ increases with increasing $A$ at the beginning of the star's evolution. If mixing is included in the region of convective turbulence only, the mass of helium synthesized during the main-sequence evolution increases with $\alpha_0$ [43]. This is not the case if intense mixing in the region of shear turbulence and the transport of hydrogen from this region into the region of convective turbulence are taken into account. If $\alpha_0$ is large, the layer of variable chemical composition is located further from the stellar center at the beginning of the main-sequence evolution. The conditions for semi-convection develop later in this case, and the contact between the semi-convective region and the region of convective turbulence occurs during later stages of the main-sequence evolution; this delay increases with increasing $\alpha_0$ (see the table). Partial mixing of the matter in the radiative envelope and the region of convective turbulence begins earlier and continues longer with decreasing $\alpha_0$. The mass of hydrogen transported from the radiative envelope into the region of convective turbulence during the evolutionary lifetime increases as $\alpha_0$ decreases. The total mass of helium synthesized during the main-sequence stage is also higher for lower $\alpha_0$. The increase in the helium mass in the outer layers brings about both an increase in the luminosity of the star and a smaller decrease in the mass of the zone where the local criterion for convective instability is valid, as well as an enhancement in the intensity of semi-convection. Therefore, at the end of the main-sequence evolution, the distance of the layer of variable chemical composition from the stellar center becomes larger with decreasing $\alpha_0$ (Fig. 4d).

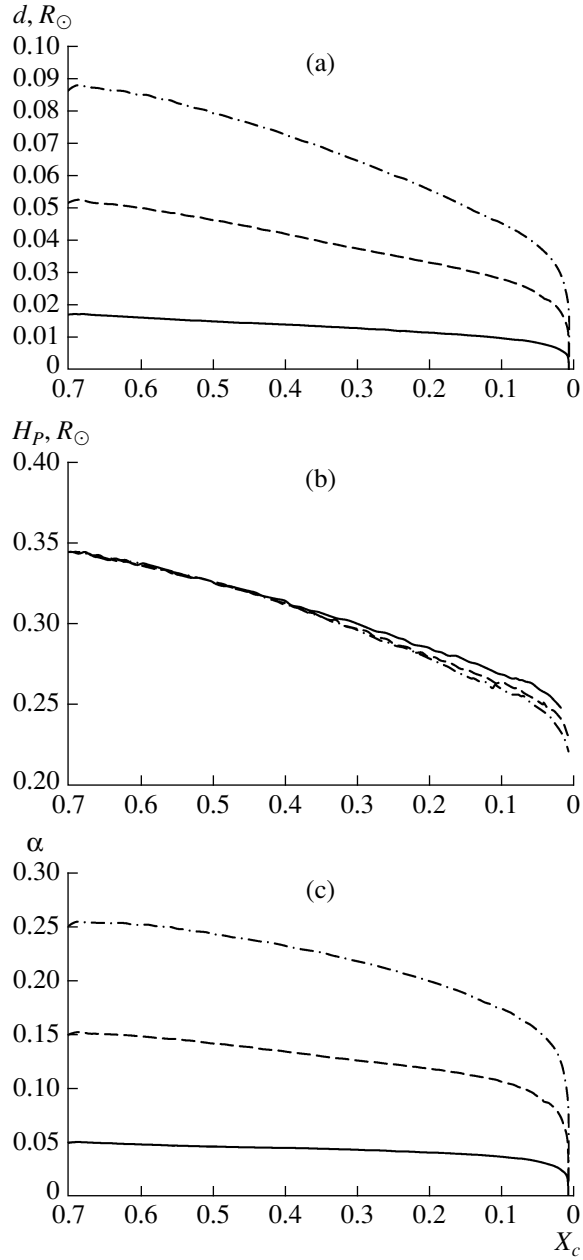


**Fig. 9.** (a) Thickness $d$ of the layer located above the region where the local criterion for convective instability is satisfied and which is mixed due to the action of turbulent entrainment. (b) Pressure scale height $H_P$ at the boundary of the region where the local criterion for convective instability is satisfied. (c) Dependence of $\alpha = d/H_P$ on the hydrogen abundance in the region of convective turbulence $X_c$ in an 8 $M_\odot$ star evolving with $\mathrm{Sc}_t = 0.1$, the S-criterion for semi-convection, and $\alpha_0 = 0.05$ (solid), $\alpha_0 = 0.15$ (dashed), and $\alpha_0 = 0.25$ (dot–dashed line).

### *4.5. Dependence of Partial Mixing on the Stellar Mass*

If the mass of the star is halved, the coefficient of turbulent diffusion decreases by an order of magnitude (Fig. 1d), while the main-sequence lifetime

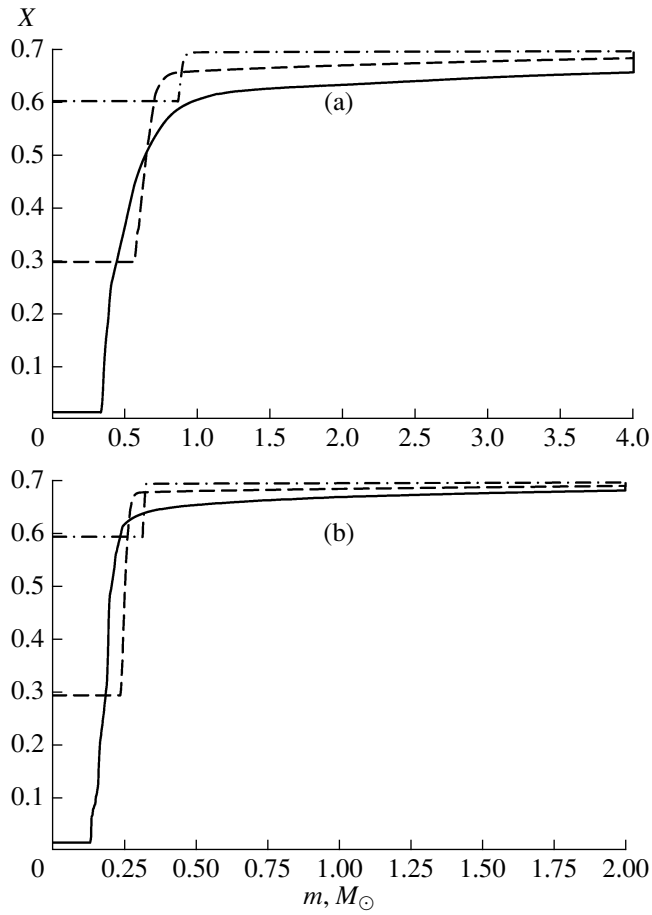


**Fig. 10.** Distributions of the hydrogen abundance in a (a) 4 $M_\odot$ and (b) 2 $M_\odot$ star when the hydrogen abundance in the region of convective turbulence is $X_c \sim 0.60$ (dot–dashed), $\sim$0.30 (dashed), and $\sim$0.02 (solid). In both cases, $\mathrm{Sc}_t = 0.1$, the S-criterion for semi-convection was adopted, and $\alpha_0 = 0.05$.

increases by about a factor of three to six (see the table). Therefore, for the given parameters of the partial-mixing model, the intensity of mixing in the region of shear turbulence decreases with decreasing stellar mass. For the development of the conditions for semi-convection, the hydrogen abundance in the layer of variable chemical composition must become higher in a lower-mass than in a higher-mass star. Thus, the conditions for semi-convection appear later if the stellar mass decreases. The contact of the semi-convective zone and the region of convective turbulence also occurs later in lower-mass stars (see the table). The fraction of mass contained in the region of convective turbulence decreases with decreasing stellar mass, while the fraction of the mass in outer layers increases. As a result, for specified parameters of the mixing model, the increase in the helium abundance in the outer layers of the star is lower for lower-mass stars (Fig. 10).

In the case of rotating 2 and 4 $M_\odot$ stars, when the equatorial angular velocity at the beginning of the main-sequence evolution is 250 km/s, the minimum angular velocity is continuously below the stellar surface during the entire main-sequence stage. The mass of the subsurface layer with angular velocity increasing outward varies from $\sim 0.1 \times 10^{-4}$ $M_\odot$ at the beginning of the main-sequence evolution of a 4 $M_\odot$ star to $\sim 4.1 \times 10^{-4}$ $M_\odot$ at the end of the evolution. For the adapted parameters of the mixing model, the ratio of the helium and hydrogen number densities in the matter below this layer increases by $\sim$22% by the end of the main-sequence evolution. An estimate of the possible loss of the sub-surface layer was made for a mass-loss rate of $1.0 \times 10^{-12}$ $M_\odot$/yr, which is close to the lower limit for the mass-loss rate according to [38]. The time scale for the loss of the sub-surface layer is shorter than the remaining main-sequence lifetime only during the first half of the main-sequence stage (Fig. 8), when the diffusion wave has not reached the stellar surface. During the second half of the star's evolution on the main sequence, when the diffusion wave appears at the stellar surface, the time required for the loss of the

sub-surface layer becomes longer than the remaining main-sequence lifetime of the star. Therefore, a discontinuity in the helium abundance forms between the sub-surface and lower layers of the star (Fig. 10). By the end of the main-sequence stage, the increase of $N_{\rm He}/N_{\rm H}$ at the surface is ~12%. If the mass-loss rate increases by more than an order of magnitude during the main-sequence stage, as is the case for the 8 $M_\odot$ star, the sub-surface layer would be lost more rapidly and the discontinuity in the helium abundance between the layers would not form. Determining the time variations of the surface helium abundance of a 4 $M_\odot$ star requires knowledge of the dependence of the mass-loss rate on the effective temperature and luminosity close to the lower boundary of the area of existence of the stellar wind.

A 2 $M_\odot$ star does not have a stellar wind. The mass of the outer layer where the angular velocity increases outward increases during the main-sequence lifetime, from $\sim 1.6 \times 10^{-4}$ to $\sim 8.3 \times 10^{-4}$ $M_\odot$. By the end of the main-sequence stage, the ratio of the helium and hydrogen number densities in the matter below this layer increases by ~8%, while it increases by ~2% in this layer itself.

## 5. THE POSSIBILITY OF INCREASING THE SURFACE HELIUM ABUNDANCES OF B0–B5 MAIN-SEQUENCE STARS

Let us consider possible increases in the surface helium abundances of early-type main-sequence B stars as a function of mixing in their interiors and their stellar-wind mass-loss.

A. *Weak mixing in the region of shear turbulence.* If the mixing in the radiative envelope is weak, the amount of hydrogen transported into the layer of variable chemical composition is small. In this case, either the conditions for semi-convection do not arise, as in the case $\mathrm{Sc}_t = 1.0$, or partial mixing of matter of the radiative envelope and the region of convective turbulence becomes possible only just before the end of the main-sequence evolution. For instance, when $\mathrm{Sc}_t = 0.3$ in an 8 $M_\odot$ star, partial mixing of the matter of the radiative envelope and region of convective turbulence begins when the hydrogen abundance in the latter has already decreased to $X_c \sim 0.20$ (see the table). The increase in $N_{\rm He}/N_{\rm H}$ in the course of the main-sequence evolution is ~0.03% for $\mathrm{Sc}_t = 1.0$ and ~4.2% for $\mathrm{Sc}_t = 0.3$ (Fig. 11a), which is less than is observed [13, 14].

B. *Evolution without semi-convection.* In this case, the initially chemically homogeneous radiative envelope of the star may mix with the layer of variable chemical composition. For an 8 $M_\odot$ star with $\mathrm{Sc}_t = 0.1$ and $\alpha_0 = 0.05$ and without semi-convection, the ratio $N_{\rm He}/N_{\rm H}$ increases by ~15% at the stellar surface by the end of the main-sequence evolution (Fig. 11a), in agreement with observational data [13, 14]. However, the hydrogen abundance in the layers located above the region of turbulence is high in this case: $X \sim 0.5$–$0.6$ (Fig. 4c). A similar hydrogen abundance can arise above the convective core of the accretor in case AB of the evolution of close binaries, due to the increase in the mass of the convective core during the accretion process [68]. With such a high hydrogen abundance, most of the energy in the helium-burning stage is released in the hydrogen-burning shell, while the mass of the helium core increases only slightly. For this reason, the accretor displays the features of a blue supergiant in the helium-burning stage. Similarly, an 8 $M_\odot$ star should display the features of a blue giant over all or most of the stage of central helium burning.

C. *Strong mixing in the region of shear turbulence with semi-convection.* In this case, the radiative envelope is partially mixed with the region of convective turbulence. As a result, the parameters of the evolution of a star on the main-sequence change, and helium is transported outward from the central regions of the star. If $Sc_t = 0.1$ and the S-criterion for convective neutrality is adopted for the semi-convective zone, the ratio $N_{\rm He}/N_{\rm H}$ at the surface of an 8 $M_\odot$ star increases by the end of the main-sequence evolution by ~80% if $\alpha_0 = 0.05$, ~50% if $\alpha_0 = 0.15$, and ~30% if $\alpha_0 = 0.25$ (Fig. 11b). When $\alpha_0 = \{0.05, 0.15\}$, the computed increase of the surface helium abundance exceeds the observed value. The increase in the mass of synthesized helium is also large: ~60–85%. When $\alpha_0 = 0.25$, the computed increase in the surface helium abundance agrees with the observations [13, 14]. The increase in the mass of synthesized helium is ~40% in this case (see the table), and either agrees with or slightly exceeds the increase required to explain the observed distribution of open-cluster stars in the Hertzsprung–Russell diagram [24]. Since the hydrogen abundance smoothly increases outward above the region of convective turbulence due to the action of semi-convection (Fig. 4d), the star will display the features of a red giant after the end of its main-sequence evolution.

D. *Evolution without mass-loss.* If there is no mass loss, $\mathrm{Sc}_t = 0.1$, the S-criterion of neutrality is adopted for the semi-convective zone, and $\alpha_0 = 0.05$, the ratio of the number densities of helium and hydrogen increases by ~23% by the end of the main-sequence evolution, in agreement with observations [13, 14]. The helium abundance in the sub-surface layer where the angular velocity increases outward grows during the evolution in this case, due to the shift of the angular-velocity minimum inward in the star and the inclusion of mixed layers located

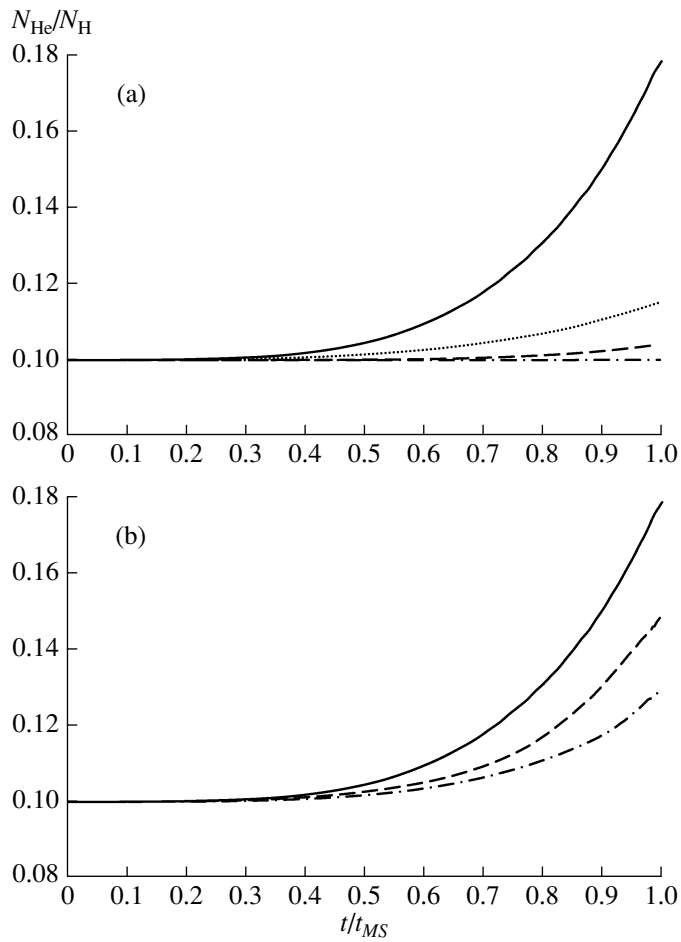


**Fig. 11.** (a) Dependence of the ratio of the helium and hydrogen number densities at the surface of an 8 $M_\odot$ star on the time during the main-sequence evolution when $\mathrm{Sc}_t = 0.1$ (solid), 0.3 (dashed), and 1.0 (dot–dashed), the S-criterion for semi-convection is applied, and $\alpha_0 = 0.05$. The case of $\mathrm{Sc}_t = 0.1$ when semi-convection is not included and $\alpha_0 = 0.05$ is also shown (dotted). (b) The same for the case $\mathrm{Sc}_t = 0.1$, with the S-criterion for semi-convection, and $\alpha_0 = 0.05$ (solid), 0.15 (dashed), and 0.25 (dot–dashed).

below the sub-surface shells into these shells. To achieve agreement between the enhancement of the helium abundance in the sub-surface layer and observations, the matter located below this layer must be strongly mixed with matter from the central regions of the star. In the case of an 8 $M_\odot$ star, such mixing results in an increase in the mass of synthesized helium by ~85%; this is much more than is required to explain the observed widths of the main sequence in open clusters [24]. Evolution without mass loss is not able to explain the enhanced helium abundances in the atmospheres of evolved main-sequence B stars.

The total mass lost by early B stars during their main-sequence lifetime is insignificant. Mass loss does not influence the structure and evolution of these stars, unlike bright main-sequence O stars. However, the change of the surface helium abundance with time is determined not only by mixing processes in the stellar interior, but also the rate of mass-loss from the outer layer, where the angular velocity grows outward. The mass of this layer is determined by the angular momentum of the star [54, 62], and is $10^{-4}$–$10^{-3}$ $M_\odot$ to order of magnitude. As computations of the evolution of an 8 $M_\odot$ star with an angular momentum of $6.94 \times 10^{51}$ erg s have shown, B0–B2 stars lose this layer via their stellar winds, over a time that is much shorter than their main-sequence lifetimes. In this case, the chemical composition of the sub-surface layer is similar to that of underlying layers. B3–B5 stars have much lower mass-loss rates, and the outer layer may be much less mixed. If the rate of stellar-wind mass loss is set equal to the minimum possible value, the value of $N_{\mathrm{He}}/N_{\mathrm{H}}$ increases by ~12% in the sub-surface layer and by ~22% in lower-lying layers of a 4 $M_\odot$ star with angular momentum $2.02 \times 10^{51}$ erg s, by the end of the main-sequence stage. The resulting variation of the surface helium abundance in B3–B5 stars is, thus,

also determined by the rate of mass loss by the stellar wind. Unfortunately, the low density stellar winds of stars close to the lower boundary of the area in which these winds can exist have not been well studied [37].

## 6. CONCLUSION

The increase in the surface helium abundances of early main-sequence B stars may be due to partial mixing of matter in the radiative envelope and the region of convective turbulence at the center of the star, as well as stellar-wind mass loss. Such partial mixing is possible if the conditions for semi-convection arise in the layer of variable chemical composition located above the region of convective turbulence, due to the transport of hydrogen from the radiative envelope into this layer via the action of shear turbulence. Shear turbulence and semi-convection are the main mechanisms bringing about partial mixing in the interiors of rotating stars. The results of partial mixing also depend on the extent to which the region involved in convective turbulence exceeds the size of the region in which the local criterion of convective instability is satisfied.

The enhancement of the surface helium abundance also depends on the rate of mass loss by the stellar wind. Since the angular-velocity minimum, where the coefficient of turbulent diffusion vanishes, is below the stellar surface, the outer layer of the star may be less mixed if the mass-loss rate is not high. The ratio of the surface number densities of helium and hydrogen increases by $\sim$30% by the end of the main-sequence evolution of an 8 $M_\odot$ star, if the parameters of the mixing model are optimal and the stellar-wind mass loss corresponds to observations. The corresponding enhancement in a 4 $M_\odot$ star can range from $\sim$12 to $\sim$22%, depending on the mass-loss rate close to the lower boundary of the area in which stellar winds can exist.

By the end of the main-sequence evolution of a 2 $M_\odot$ star with an angular momentum of $0.55 \times 10^{51}$ erg s, the enhancement of $N_{\rm He}/N_{\rm H}$ is $\sim$2% in the sub-surface layer and $\sim$8% below this layer. The errors in observational estimates of helium abundances are such that the variations in the surface helium abundances in stars of this mass may be undetectable. In the absence of stellar wind, the upper, less mixed layer may hide mixing processes occurring in the interiors of such stars.

## REFERENCES


1. A. G. Masevich and A. V. Tutukov, *Stellar Evolution: Theory and Observations* (Nauka, Moscow, 1988) [in Russian].
2. G. S. Bisnovatyi-Kogan, *Physical Problems in the Theory of Stellar Evolution* (Nauka, Moscow, 1989) [in Russian].
3. G. S. Bisnovatyi-Kogan, *Stellar Physics. I. Fundamental Concepts and Stellar Equilibrium* (Springer, Heidelberg, 2001).
4. M. Asplund, N. Grevesse, and A. J. Sauval, in *Cosmic Abundances as Record of Stellar Evolution and Nucleosynthesis*, Ed. by F. N. Bash and T. G. Barnes, ASP Conf. Ser. **336**, 25 (2005).
5. J. C. Howk, K. R. Sembach, and B. D. Savage, Astrophys. J. **543**, 278 (2000).
6. C. R. Proffitt and M. F. Quigley, Astrophys. J. **548**, 429 (2001).
7. K. A. Venn, A. M. Brooks, D. L. Lambert, M. Lemke, N. Langer, and D. J. Lennon, Astrophys. J. **565**, 571 (2002).
8. J. T. Mendel, K. A. Venn, and C. R. Proffitt, Astrophys. J. **640**, 1039 (2006).
9. J. Fliegner, N. Langer and K. A. Venn, Astron. Astrophys. **308**, L13 (1996).
10. L. S. Lyubimkov, Sov. Astron. Lett. **1**, 14 (1975).
11. L.S. Lyubimkov, in *Chemical Evolution of Stars and Galaxies,* Collection of Articles (Kosmosinform, Moscow, 1992), p. 64 [in Russian].
12. L.S. Lyubimkov, *Chemical Structure of Stars: Method and Results of Analysis* (Astroprint, Odessa, 1995) [in Russian].
13. L. S. Lyubimkov, S. I. Rostopchin, and D. L. Lambert, Mon. Not. R. Astron. Soc. **351**, 745 (2004).
14. W. Huang and D. R. Gies, Astrophys. J. **648**, 591 (2006).
15. A. Herrero, R. P. Kudritzki, J. M. Vilchez, D. Kunze, K. Butler, and S. Haser, Astron. Astrophys. **261**, 209 (1992).
16. A. Herrero, L. J. Corral, M. R. Villamaris, and E. L. Martin, Astron. Astrophys. **348**, 542 (1999).
17. A. Herrero, J. Puls, and M. R. Villamaris, Astron. Astrophys. **354**, 193 (2000).
18. K. Hunger and D. Groote, Astron. Astrophys. **351**, 554 (1999).
19. J. I. Castor, D. C. Abbott, and R. I. Klein, Astrophys. J. **195**, 157 (1975).
20. J. Krtička and J. Kubát, Astron. Astrophys. **369**, 222 (2001).
21. J. Krtička and J. Kubát, Astron. Astrophys. **377**, 175 (2001).
22. J. Krtička, J. Kubát, and D. Groote, Astron. Astrophys. **460**, 145 (2006).
23. A. Maeder, Astron. Astrophys. **32**, 177 (1974).
24. A. Maeder and J.-C. Mermilliod, Astron. Astrophys. **93**, 136 (1981).
25. G. Meylan and A. Maeder, Astron. Astrophys. **108**, 148 (1982).
26. J.-C. Mermilliod and A. Maeder, Astron. Astrophys. **158**, 45 (1986).
27. C. A. Meakin and D. Arnett, Astrophys. J. **667**, 448 (2007).
28. M. Schwarzshild and R. Harm, Astrophys. J. **128**, 348 (1958).
29. A. S. Eddington, Observatory **48**, 73 (1925).

30. H. Vogt, Astron. Nachr. **223**, 229 (1925).
31. J.-P. Zahn, Astron. Astrophys. **265**, 115 (1992).
32. S. Ekström, G. Georgy, P. Eggenberger, G. Meynet, Mowlavi, N. Mowlavi, A. Wyttenbach, A. Granada, T. Decressin, R. Hirschi, U. Frischknecht, C. Charbonnel, and A. Maeder, Astron. Astrophys. **537**, 146 (2012).
33. U. Frischknecht, R. Hirsci, G. Meynet, S. Ekström, C. Georgy, T. Rauscher, C. Winteler, and F.-K. Thielemann, Astron. Astrophys. **522**, 39 (2010).
34. N. Przybilla, M. Firnstein, M. F. Nieva, G. Meynet, and A. Maeder, Astron. Astrophys. **517**, 38 (2010).
35. J. S. Vink, A. de Koter, and H. J. G. L. M. Lamers, Astron. Astrophys. **362**, 295 (2000).
36. G. Georgy, S. Ekström, G. Meynet, P. Massey, E. M. Levesque, R. Hirschi, P. Eggenberger, and A. Maeder, Astron. Astrophys. **542**, 29 (2012).
37. J. Puls, J. S. Vink, and F. Najarro, Astron. Astrophys. Rev. **16**, 209 (2008).
38. J. Krtička, Astron. Astrophys. **564**, 70 (2014).
39. J.-P. Zahn, Mem. Soc. R. Sci. Liège **8**, 31 (1975).
40. D. Arnett, C. A. Meakin, and P. A. Young, Astrophys. J. **690**, 1715 (2009).
41. M. Viallet, C. Meakin, D. Arnett, and M. Mocak, Astrophys. J. **769**, 1 (2013).
42. C. A. Meakin and D. Arnett, Astrophys. Space Sci. **328**, 221 (2010).
43. E. I. Staritsin, Astron. Rep. **57**, 380 (2013).
44. J.-L. Tassoul, *Stellar Rotation,* Cambridge Astropysics, Vol. 36 (Cambridge Univ. Press, 2000; Mir, Moscow, 1982).
45. A. Maeder and J.-P. Zahn, Astron. Astrophys. **334**, 1000 (1998).
46. S. Kato, Publ. Astron. Soc. Jpn. **18**, 374 (1966).
47. S. Sakashita and C. Hayashi, Progr. Theor. Phys. **26**, 942 (1961).
48. P. Ledoux, *Stellar Stability* (Springer, Berlin, 1958).
49. E. I. Staritsin, Astron. Lett. **35**, 413 (2009).
50. B. Chaboyer and J.-P. Zahn, Astron. Astrophys. **253**, 173 (1992).
51. E. V. Bruyatskii, *Turbulent Stratified Jet Flows* (Naukova Dumka, Kiev, 1986) [in Russian].
52. *Prediction Methods for Turbulent Flows*, Ed. by W. Kollman (Hemisphere, 1980; Mir, Moscow, 1984).
53. S. Talon and J.-P. Zahn, Astron. Astrophys. **317**, 749 (1997).
54. S. Talon, J.-P. Zahn, A. Maeder, and G. Meynet, Astron. Astrophys. **322**, 209 (1997).
55. A. Maeder, Astron. Astrophys. **399**, 263 (2003).
56. S. Mathis, A. Palacios, and J.-P. Zahn, Astron. Astrophys. **425**, 243 (2004).
57. H. J. S. Fernando, Ann. Rev. Fluid Mech. **23**, 455 (1991).
58. C. de Jager, H. Nieuwenhuijzen, and K. A. van der Hucht, Astron. Astrophys. Suppl. Ser. **72**, 259 (1988).
59. B. Paczynski, Acta Astron. **20**, 47 (1970).
60. E. I. Staritsin, Astron. Rep. **43**, 592 (1999).
61. E. I. Staritsin, Astron. Rep. **49**, 634 (2005).
62. E. I. Staritsin, Astron. Lett. **33**, 93 (2007).
63. C. A. Iglesias and F. J. Rogers, Astrophys. J. **464**, 943 (1996).
64. D. R. Alexander and J. Ferguson, Astrophys. J. **437**, 879 (1994).
65. I. Yimer, I. Campbell, and L.-Y. Jiang, Canad. Aeronaut. Space J. **48**, 195 (2002).
66. E. I. Staritsin, Astron. Rep. **45**, 467 (2001).
67. L. D. Landau and E. M. Livshitz, *Fluid Mechanics* (Nauka, Moscow, 1986; Pergamon, New York, 1987).
68. E. I. Staritsin, Astron. Rep. **40**, 773 (1996).

*Translated by L. Yungel'son*